SPEAR3 COMMISSIONING

J. Safranek*, S. Allison, P. Bellomo, W.J. Corbett, M. Cornacchia, E. Guerra, R. Hettel, D. Keeley, N. Kurita, D. Martin, P. McIntosh, H. Morales, G. Portmann, F. Rafael, H Rarback, J. Sebek, T. Straumann, A. Terebilo, J. Wachter, C. Wermelskirchen, M. Widmeyer, R. Yotam (SSRL/SLAC, Stanford, CA, USA); M.H. Yoon (PAL, Korea); J. Byrd, D. Robin, T. Scarvie, C. Steier (ALS, USA); L. Nadolski (SOLEIL, France); H.P. Chang, C.C. Kuo, H.J. Tsai (NSRRC, Taiwan); S. Krinsky, B. Podobedov (NSLS/BNL, USA); W. Decking (DESY, Germany); M. Boege (SLS, Switzerland); A. Ropert (ESRF, France); M. Boland, E. Tan (ASP, Australia); M. Fedurin, P. Jines (CAMD, USA); K. Harkay, V. Sajaev (APS, USA)

Abstract

The successful commissioning of the new SPEAR3 light source at the Stanford Synchrotron Radiation Laboratory (SSRL) will be reviewed. Orbit control, beam-based alignment, and an orbit interlock were commissioned. Orbit motion was characterized as a function of frequency. The linear optics was corrected for ID focusing and coupling errors. The nonlinear optics were investigated with dynamic aperture measurements as a function of energy and tune. Preliminary measurements were made of impedances and instabilities.

INTRODUCTION

The SPEAR storage ring was built in 1972 as an e-/e+ collider at Stanford Linear Accelerator Center. In 1989 it became a fully dedicated synchrotron light source for SSRL. The SPEAR3 project is a complete rebuild of the SPEAR storage ring, from a new concrete tunnel floor up [1]. The new storage ring maintained only the original geometry, rebuilding the 18 cells of the ring about the existing 7 insertion devices and 4 dipole beamlines. SPEAR3 provides higher brightness, increased stored current, and better beam stability. The horizontal emittance has been reduced by nearly a factor of ten to 18 nm*rad, and the storage ring is capable of storing up to 500 mA.

Because SSRL was an operating light source with an active user community prior to SPEAR3, a speedy installation and commissioning was essential. The entire process lasted 11 months, with removal of the old SPEAR storage ring starting on March 31, 2003. Eight months later, on December 9, SPEAR3 started a three-month commissioning period. First beam to SPEAR3 was on December 10, with first accumulated beam on December 15. On January 22, 100 mA was stored, and March 15 saw the start of user operations.

The commissioning team included experts visiting from light source laboratories worldwide. The visitors typically came for periods of a week or two, and their experience and expertise helped to ensure rapid commissioning success.

CONTROL SYSTEM

A flexible and adaptable MATLAB interface to an EPICS control system enabled the commissioning group to quickly develop code for beam dynamics measurements and to rapidly respond to issues arising while commissioning the various storage ring systems. This MATLAB code was ported from the ALS [2] with many improvements made for SPEAR3 [3]. Measurement data going directly to MATLAB greatly facilitated data analysis and plotting. The MATLAB interface enabled us to gather and analyze a remarkable quantity of data during commissioning and to gain a thorough understanding of the storage ring within a short time.

A web-based electronic logbook [4] was used to record commissioning results. In this way the team was easily kept up to date on commissioning issues and progress.

* safranek@slac.stanford.edu

DIAGNOSTICS

The diagnostics available during commissioning were a Bergoz DCCT, a stripline tune driver, and 112 BPMs, 54 of which had Bergoz electronics [5]. In the coming months we expect to bring online the first set of 18 Echotek [6] BPM electronics with digital receivers, capable of turn-by-turn as well as low-noise closed orbit measurements. In addition, we will have an x-ray pinhole camera [7], a UV synchrotron light monitor [8], and horizontal and vertical scrapers.

The measured noise from the DCCT is 1 μA rms with 0.5 second averaging. This noise level is independent of stored current

The BPM orbit readings are updated at 4 kHz. For closed orbit measurements, we typically average 0.5 seconds of data (2000 consecutive readings). The typical rms variation for 0.5 second data is 100 nm, most of which can be attributed to real orbit motion. The noise level for 4 kHz data is about 5 microns.

COMMISSIONING RESULTS

Closed orbit

The measured closed orbit with all steering magnets turned off has peaks under 4 mm horizontally and 2 mm vertically. The relatively small closed orbit shows that the ring is well aligned.

Beam-based alignment was used to determine the BPM offsets [9]. Figure 1 shows beam-based alignment data for one BPM, BPM(2,4). The plot has 54 curves, one for each of the 54 BPMs. The five points on each curve are for five different closed orbits in BPM(2,4). For each

closed orbit, the strength of the quadrupole adjacent to BPM(2,4) is changed, and the shift in orbit at the 54 BPMs is recorded. The average of the zero intercepts gives the offset of BPM(2,4) from the adjacent quadrupole center.

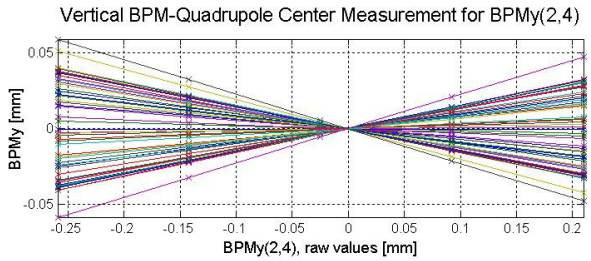

Figure 1: Vertical beam-based alignment data for one BPM.

Beam-based alignment analysis determined that the combined mechanical and electrical BPM offsets for the 54 BPMs in both planes were 0.7 mm or less. The reproducibility of the beam-based alignment was 2 μm rms for data sets taken 3 hours apart, and 23 μm rms for data sets taken 38 days apart.

An orbit interlock protects the vacuum chamber from mis-steering of high power insertion device (ID) radiation. The orbit is monitored on BPMs upstream and downstream of each ID. If the orbit at the center of the ID (y, y') gets beyond the trip level,

$$\frac{|y|}{1.2\,mm} + \frac{|y'|}{0.36\,mrad} < 1 \qquad (1)$$

the beam is dumped within 2 msec.

Orbit drift

The orbit stability specification for SPEAR3 is <10% of the beam size, which comes to 3-5 microns vertically and 16-43 microns horizontally, depending on the beamline source point. Great effort was made in the SPEAR3 design to minimize orbit motion [1].

During commissioning, measurements were made to characterize both the slow orbit drift and the orbit motion at frequencies above 1 Hz. The orbit drift over the course of 10 hours with no orbit feedback had peaks of about 100 μm in x and 50 μm in y.

This measured orbit drift is a combination of real orbit motion and apparent motion associated with BPM errors such as mechanical BPM movement, electronics drift or intensity dependence. The former can be readily corrected with orbit feedback, while the latter is more problematic and often defines the limit of orbit stabilization.

Expanding the orbit drift in orbit response matrix eigenvectors showed that most of the orbit motion was in the eigenvectors with the largest singular values. This indicates that the measured motion was primarily real motion, with at most a small fraction due to BPM errors.

In order to further characterize apparent orbit drift associated with BPM errors, beam-based measurements were made of electronics intensity dependence. The measured orbit shift between 100 mA and 50 mA (the typical range of currents that will be used in the first year of operations) was 3.4 μm rms in x and 3.0 μm in y.

Orbit jitter

The power spectral density was derived from the 4 kHz BPM data. The measured PSD for orbit jitter between 2 and 200 Hz integrates to 3.7 μm horizontally (Fig. 2) and 2.2 μm vertically. This is within the orbit stability specification.

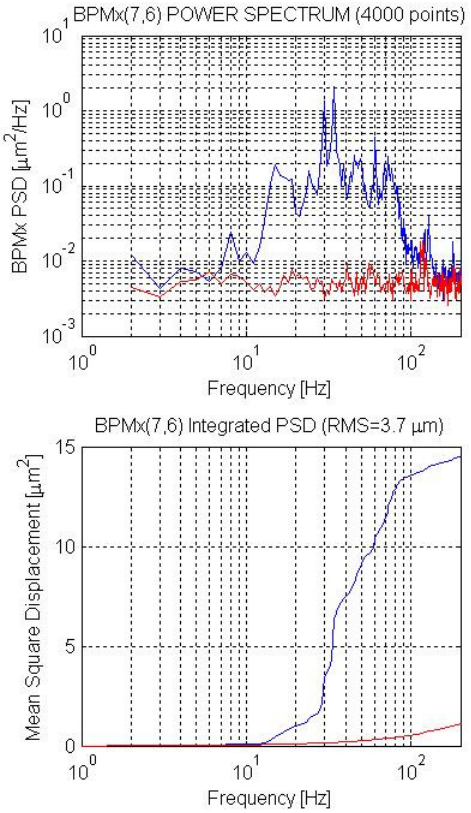

Figure 2: Horizontal PSD and PSD integral. Blue is measured orbit motion; red is measured BPM noise floor.

Orbit feedback

A MATLAB-based slow orbit feedback which corrects the orbit every six seconds was implemented for the start of operations. The feedback uses all 54 steering magnets in each plane and holds the measured orbit shift at the 54 Bergoz BPMs to better than 1 μm over the course of a fill.

The hardware is in place for a digital fast orbit feedback using the 4 kHz BPM data to correct orbit motion out to ~200 Hz. This system will be commissioned during the first year of operation.

Optics

Most of the optics characterization and correction was done by analyzing closed orbit response matrix data with the LOCO code [10]. We determined that the initial .017 error in the measured vertical tune is primarily associated with excess focusing in the dipole magnets. LOCO was

also used to calibrate and correct the beta and dispersion functions, calibrate the BPM gains and steering magnet strengths, correct the coupling and vertical dispersion, and measure the local chromaticity and transverse impedance distributions.

The top half of Fig. 3 shows the vertical beta function distortion with insertion devices closed. The vertical beta function was found using LOCO to fit the AT [11] model to the measured response matrix. The fit model was then used to determine quadrupole gradient changes that best corrected the optics distortion. The bottom half of Fig. 3 shows the vertical beta function fit to the response matrix measured after applying this correction.

The vertical beam size was minimized by correcting the off-diagonal elements of the orbit response matrix and the vertical dispersion [12]. SPEAR3 has skew quadrupole windings on each sextupole. Fourteen of the skew windings are powered. LOCO was used to find the strengths of the 14 skew quadrupoles that minimize the off-diagonal (coupling) parts of the orbit response matrix and minimize the measured vertical dispersion. We had no vertical beam size measurement to check the correction. Instead, we put 19 mA in a single bunch to get in the Touschek lifetime regime, then put in and out the coupling correction. The correction decreased the lifetime from 4.3 hours to 1.8 hours.

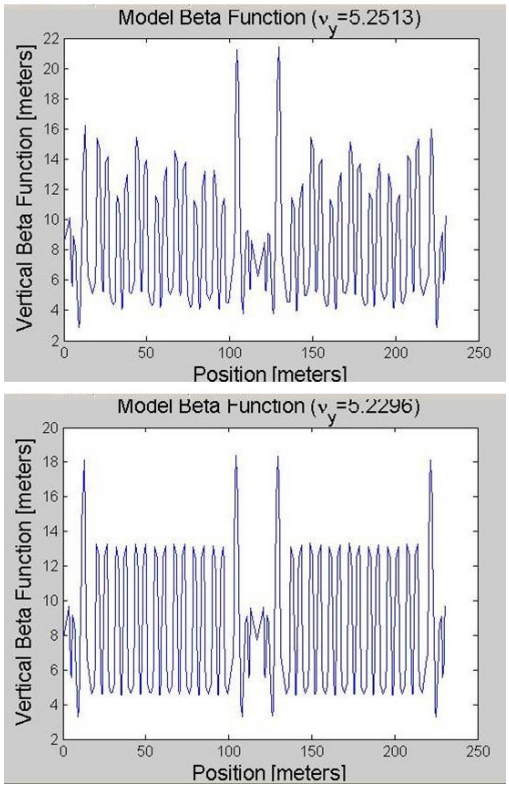

Figure 3: Vertical beta function from model fit to response matrix before (above) and after correction.

Optics upgrade study

The horizontal emittance was reduced from 18 to 12 nm*rad by permitting finite (10 cm) horizontal dispersion in the ID straight sections. This optics was implemented using LOCO. Figure 4 shows the measured horizontal dispersion in the nominal and low emittance optics. In the low emittance optics, we found that the dynamic aperture was sufficient for good injection and that the lifetime was slightly longer than in the nominal optics. The low emittance optics is reserved as a future upgrade.

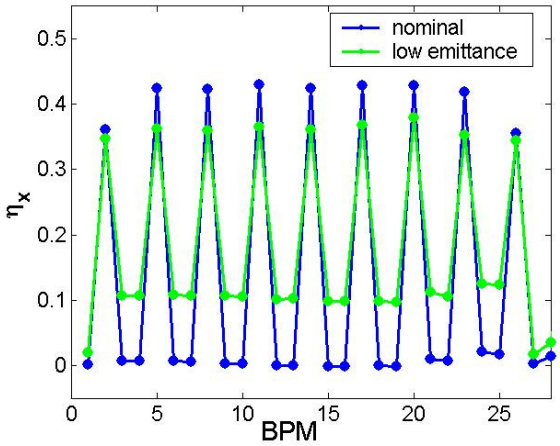

Figure 4: Comparison of the measured horizontal dispersion in the nominal and low emittance optics.

Nonlinear transverse dynamics

To characterize the nonlinear dynamics, we measured the local chromaticity correction, the nonlinear chromaticity, the dynamic aperture as a function of RF frequency and as a function of transverse tunes, the lifetime as a function of RF gap voltage and as a function of transverse tunes, and the lifetime as a function of vertical physical aperture.

The local chromaticity correction was verified by measuring two orbit response matrices, one with the RF frequency set at +5 kHz and one at -5 kHz from nominal. Each response matrix was fit with LOCO to get the betatron phase advance around the ring. The difference in phase advance gives the local chromaticity. This measurement confirmed that the sextupoles are all working correctly.

The measured nonlinear chromaticity over the full energy range also showed good agreement with the model.

Figure 5 shows the measured horizontal dynamic aperture as a function of energy with insertion devices closed. With IDs open, the dynamic aperture was about 20% larger. The data was taken by filling 1 mA, then increasing the strength of single injection kicker until the beam was kicked out of the ring. This was repeated for varying RF frequency. The height of each bar gives the point at which the beam was lost for that energy (RF frequency).

The blue curves plotted in Fig. 5 give the horizontal oscillation amplitude that would be excited for the given energy shift, depending on where in the ring the energy shift occurred. Each straight section has a different blue curve, depending on the nonlinear dispersion and beta functions. The intersection of the blue curves and the

dynamic aperture curves give the dynamic energy aperture [13].

The measured dynamic apertures are on the order of 10% larger than expected from tracking results. This could be due to calibration uncertainties in the kickers. Once the turn-by-turn BPMs are commissioned, we will calibrate the oscillation amplitude vs. kicker strength.

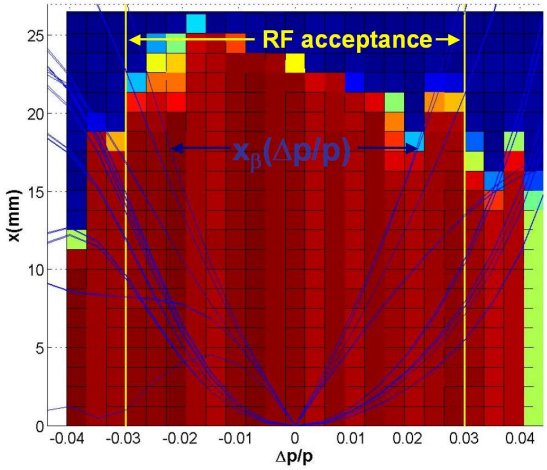

Figure 5: Measured horizontal dynamic aperture vs. energy, IDs closed.

The dynamic energy aperture was also determined by measuring the lifetime vs. RF gap voltage. The measurement was made with 8 mA in a single bunch to get in the Touschek lifetime regime, where the cubed root of the lifetime scales linearly with the rf acceptance.

Figure 6 shows a plot of the data along with a fit line giving the Touschek scaling. The data deviates from Touschek scaling at low gap voltages, where quantum lifetime effects become significant. The data starts to diverge from the line for increasing energy acceptance at about 2%. This indicates that the dynamic energy acceptance is 2% for some of the straight sections, consistent with the results in Fig. 5.

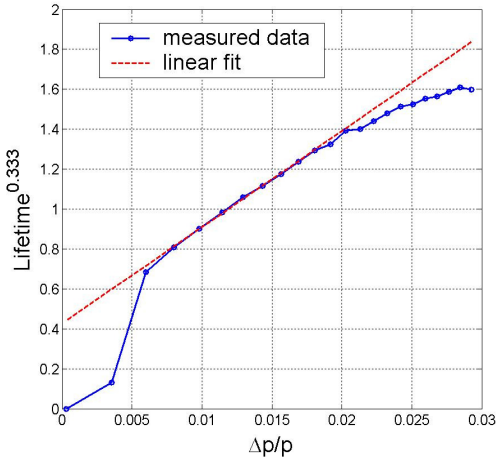

Figure 6: Cubed root of lifetime vs RF energy acceptance, ID gaps closed.

Figure 7 shows the measured dynamic aperture as a function of horizontal and vertical tune. This data was collected automatically over the course of several hours using a MATLAB script. For each data point, 1 mA was injected, the tunes were adjusted to a point on a grid, and a single injection kicker strength was raised until the stored beam was kicked out.

Figure 7 shows some resonant features. The dynamic aperture decreases along the difference coupling resonance, and along the $3\nu_x+\nu_y$ resonance. The reduction in dynamic aperture along the $3\nu_x+\nu_y$ resonance is offset from the resonance line due to the tune shift with amplitude. The zigzag along this resonance is simply a plotting feature associated with the density of data points.

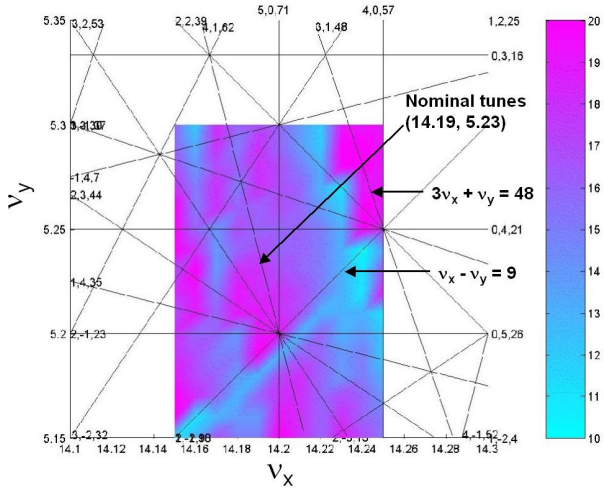

Figure 7: Measured dynamic aperture (maximum kicker strength) vs. transverse tunes.

The measurement in Fig. 7 is an example of the strength of the MATLAB environment for accelerator control. The script was written, debugged and running within a couple hours, and it collected the data over several hours with no human intervention required.

The lifetime was also measured as a function of transverse tunes. Lifetime degradation was seen along the difference resonance. The measurement showed that the chosen working point for the tunes gives good lifetime.

Longitudinal dynamics

When injection was first attempted in SPEAR3, all sextupoles were left off. The assumption was that on day one, the closed orbit errors would be large. Large orbit distortions in the sextupoles distort the transverse optics and degrade the dynamic aperture. So sextupoles were left off to improve the transverse dynamics.

We had difficulty storing beam with sextupoles off. Tracking studies of the longitudinal dynamics showed that the acceptance is greatly reduced without sextupoles, due to a large increase in the second order momentum compaction factor, α_2. Figure 8 shows measurements of α_2 with and without sextupoles. The large increase in α_2 with sextupoles off was confirmed.

Lifetime & vacuum pressure

The vacuum pressure has decreased with beam scrubbing to <2 nTorr average pressure. The beam lifetime has steadily increased to 26 hours at 100 mA after

90 A*hours of total integrated stored beam. We anticipate that the lifetime will eventually reach ~18 hours with 500 mA stored.

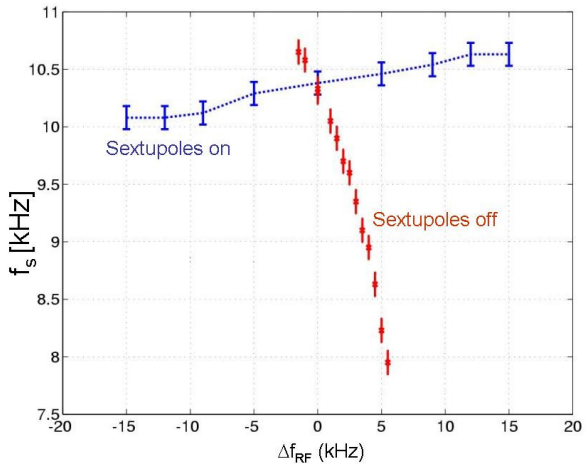

Figure 8: Measured second order momentum compaction factor.

Impedances & instabilities

During the commissioning period, radiation protection requirements prohibited us from injecting more than 100 mA. SPEAR3 was designed for 500 mA, and we hope to attempt to fill to 500 mA sometime during the first year of operation.

With 100 mA stored, we initially saw spontaneous excitation of vertical betatron oscillations. The oscillations, however, were at the mode frequencies associated with ion instabilities, and they have all but disappeared as the vacuum has improved.

We also see some excitation of longitudinal oscillations. Rather than beam instabilities, these appear to be driven oscillations (probably by the RF), which we will work to eliminate.

With the chromaticities corrected to +1 in each plane, the single-bunch stored current limit is 25 mA.

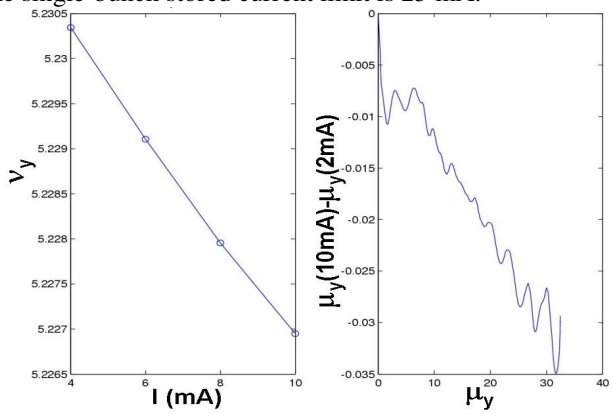

Figure 9: Vertical transverse impedance measurement. Left, tune vs. current; right, local phase advance change.

Orbit response matrices were measured as a function of single bunch current and analyzed with LOCO to find the change in betatron phase advance around the ring as a function of current (see Fig. 9). This gives a measure of the transverse impedance distribution [14].

CONCLUSION

The control system and diagnostics available for SPEAR3 commissioning enabled the commissioning team to gather and analyze a substantial amount of data in a relatively short time. After only three months, the SPEAR3 storage ring orbit, optics, and nonlinear dynamics have been well characterized and controlled.

ACKNOWLEDGEMENTS

We would like to commend the SPEAR3 staff for their work during and before commissioning. The speed at which commissioning proceeded is a testimony to the fine work that went into designing and building SPEAR3. The experience and energy of the SSRL operations group was also a great benefit during commissioning.

Many thanks to P. Krejcik for setting up the electronic logbook and helping this valuable tool run smoothly.

This research was carried out at the Stanford Linear Accelerator Center, a national user facility operated by Stanford University on behalf of the U.S. Department of Energy, and was supported by the DOE Office of Science.

REFERENCES

[1] R. Hettel et al., "SPEAR3 upgrade project: the final year", PAC 2003.
"SPEAR3 design report", SLAC-R-069, 1999.
[2] Portmann, "Slow orbit feedback at the ALS using MATLAB", PAC 1999.
[3] W.J. Corbett et al., "SPEAR3 Commissioning Software", to be published, EPAC 2004.
[4] K. Rehlich and R. Kammering, http://tesla.desy.de/doocs/doocs.html.
[5] http://www.bergoz.com/
[6] http://www.echotek.com/ecdr_814.asp.
[7] C. Limborg et al., "A pinhole camera for SPEAR2", EPAC 2000.
[8] C. Limborg et al., "An Ultra-Violet Light Monitor for SPEAR3", EPAC 2002.
[9] G. Portmann and D. Robin, "Beam-based alignment of C-shaped quadrupole magnets", EPAC 1998.
[10] J. Safranek, G. Portmann, A. Terebilo, C. Steier, "MATLAB-based LOCO", EPAC 2002. http://ssrl.slac.stanford.edu/loco/.
[11] http://www-ssrl.slac.stanford.edu/at/.
[12] J. Safranek, S. Krinsky, PAC 1993, pg. 1491.
[13] C. Steier, D. Robin, L. Nadolski, W. Decking, Y. Wu, and J. Laskar, "Measuring and optimizing the momentum aperture in a particle accelerator", Phys. Rev. E, vol. 65 no. 056506 (May, 2002).
[14] V. Sajaev, "Transverse impedance distribution measurements using the response matrix fit method at APS", PAC 2003.